JOURNAL OF SOLID STATE CHEMISTRY 111, 33–40 (1994)

Synthesis and Characterization of NZP Phases, $AM'^{3+}M''^{4+}P_3O_{12}$[1]

M. Sugantha and U. V. Varadaraju

Materials Science Research Centre, Indian Institute of Technology, Madras 600 036, India

and

G. V. Subba Rao

Central Electrochemical Research Institute, Karaikudi 623 006, India

Received October 25, 1993, accepted February 7, 1994

DEDICATED TO PROFESSOR C. N. R. RAO ON HIS 60TH BIRTHDAY

A wide variety of isostructural phases of the NZP family, $AM'^{3+}M''^{4+}P_3O_{12}$, have been synthesized. Some of these phases are reported for the first time. Characterizations by IR, EPR, and UV–visible spectroscopic methods are presented. DC magnetic susceptibility measurements on selected phases show antiferromagnetic ordering of $AZrFeP_3O_{12}$ (A = Sr, Ba) phases. © 1994 Academic Press, Inc.

INTRODUCTION

Compounds based on sodium zirconium phosphate, $NaZr_2P_3O_{12}$, popularly known as NZP phases (general formula $A^{+1}M_2^{4+}P_3O_{12}$), have evoked considerable interest in the past several years because of their potential applications including fast ion conduction (1–3). They exhibit a hexagonal crystal structure (4) with a space group $R\bar{3}C$ with six formula units per unit cell. The crystal structure can be described as a network formed by the corner sharing of PO_4 tetrahedra and MO_6 octahedra. The basic unit of the framework consists of two MO_6 octahedra and three PO_4 tetrahedra which are linked along the c-axis. Such ribbons along the c-axis are interconnected by PO_4 tetrahedral units along the a-axis. The articulation of these ribbons and chains creates structural holes or interstitial sites in the structure which can accommodate a variety of A ions. There are four such sites per formula unit of the NZP, as represented by the crystallographic formula $(A_I)(A_{II})_3M_2(PO_4)_3$. The A_I and the A_{II} sites have different crystallographic orientations. The A_I (type I) sites are situated between two MO_6 octahedra along the c-axis with a distorted octahedral coordination, while the A_{II} (type II) sites are located between the ribbons with an eight-fold coordination. In NZP the Na ion occupies only the type I (6b) sites while the type II (18e) sites are empty. In $Na_4Zr_2(SiO_4)_3$, the A_I and *all* the A_{II} sites are filled. In this process of increasing Na content, the network structure comprising interlinked ZrO_6 and PO_4 and/or SiO_4 tetrahedra remains intact, but the structure changes from a hexagonal to a monoclinic lattice. This rigid framework structure also allows either nil occupancy as in $\square NbTiP_3O_{12}$ or partial occupancy as in NZP and NASICON ($Na_3Zr_2Si_2PO_{12}$). Thus, NZP offers an open structure with rigid framework and vacant interstitial sites which can be filled by metal ions.

The NZP structure is versatile in that chemical substitution is possible at the A, M, and P sites by a variety of elements to give rise to a large number of isostructural phases, including vacancy at the A site (5–11). The substitution at the Na site includes alkali and alkaline earth metals, rare earths (x = 0.33), thallium, silver, copper, ammonium ion, and zirconium (x = 0.25). The two available Zr sites can be occupied simultaneously by M^{5+} and M^{4+} ions, leaving A site vacant. The phosphorus site can be substituted partially or fully by Si or As. It is also possible to replace Zr by trivalent ions such as Fe, Cr, Ga, etc., which can retain octahedral coordination. Maintaining the charge neutrality conditions, compounds of the type $AM'^{3+}M''^{4+}P_3O_{12}$ (A = Ca, Sr, Ba; M'^{3+} = Cr, Fe, Ga; M''^{4+} = Ti) have also been prepared (5). Recently, mixed valent compounds of the type $ATi^{3+}Ti^{4+}P_3O_{12}$ (A = Ca, Sr, Ba) and $\square Nb^{4+}Nb^{5+}P_3O_{12}$ have been prepared and the isostructural nature of the phases has been established (11, 12).

In cases where M' and M'' ions can have variable valency it is possible to do interesting soft chemistry to prepare Li and Na intercalated compounds; compounds are also obtained by deintercalation (9). Thus, NZP framework provides ample scope for tailoring physical proper-

[1] Forms part of the Ph.D. thesis to be submitted by M. Sugantha to the Indian Institute of Technology, Madras.

0022-4596/94 $6.00

ties such as ionic conductivity (1–3), thermal expansion coefficient (13, 14), dielectric properties, and establishment of crystal structure–property correlations.

The present study deals with the synthesis and characterization of NZP phases of the type $AM'^{3+}M''^{4+}P_3O_{12}$ (A = Ca, Sr, Ba; M'^{3+} = Ti, Cr, Fe, In; M''^{4+} = Ti, Zr). Some of these phases are reported in the literature; but detailed spectroscopic characterization studies have not been reported. These phases are characterized by XRD, UV–visible, IR, and EPR studies. The temperature dependence of magnetic susceptibility has been studied for selected samples.

EXPERIMENTAL

The compounds $AM'^{3+}M''^{4+}P_3O_{12}$ (A = Ca, Sr, Ba, M'^{3+} = Cr, Fe, In, and M''^{4+} = Ti, Zr) were prepared by high temperature solid state reaction in air starting from high purity metal oxides/carbonates and $NH_4H_2PO_4$. The final sintering was done at 1100°C. Mixed valent compounds of the type $AM^{3+}M^{4+}P_3O_{12}$ (M = Ti) and $M^{5+}M^{4+}P_3O_{12}$ (M = Nb) were prepared by adopting a slightly different procedure (11, 14). Mixtures of alkaline earth metal carbonates, $NH_4H_2PO_4$ and TiO_2 or Nb_2O_5 were mixed thoroughly and heated in air at 300°C for 10–12 hr, 600°C for 24 hr and 900°C for 24 hr with several intermittant grindings. The required quantity of metallic Ti/Nb was added to give the stoichiometric formula to the above master composition, mixed thoroughly, and pelletized. The pellets were then heated in an evacuated ($\sim 10^{-5}$ Torr) and sealed quartz tube at 1100°C for 24 hr and cooled. This process was repeated one more time with a third and final sintering at 1200°C for 3 hr.

The phases were characterized by powder X-ray diffraction (Rich Seifert, Germany, XRD-3000P, 35 kV, 30 mA, Cu$K\alpha$ radiation). The hexagonal lattice parameters were obtained by an LSQ fit of the high angle lines. The densities of the samples were measured at room temperature by pycnometry using xylene. The thermal stability studies were done on select samples using TGA/DTA (Netzch) Germany, STA 409).

Infrared spectra were recorded in the range 1400–200 cm^{-1} as KBr pellets or polyethelene discs (Perkin Elmer 983). UV–visible spectra on select samples were recorded as powders in the range 2000–200 nm using a Varian Cary 2300 spectrophotometer. DC magnetic susceptibility measurements (χ–T) were carried out on Fe-containing and mixed valent Ti phases in the temperature range 350–1 K using a commercial SQUID magnetometer (Quantum Design, USA, Model 1822, MPMS) at a field of 1000 G. The EPR measurements on the mixed valent Ti and Nb compounds were made at room temperature and at liquid N_2 temperature (Varian E-112, X band frequency).

RESULTS AND DISCUSSION

A. Phase Formation, Structure, and Stability

A large number of compounds of the type $AM'^{3+}M''^{4+}P_3O_{12}$, where A = Ca, Sr, Ba; (M'^{3+}, M''^{4+}) = (Ti, Ti), (Cr, Ti), (Fe, Ti), (Cr, Zr), (Fe, Zr), (In, Zr), and $\square M^{5+}M^{4+}P_3O_{12}$, where ($M^{5+}M^{4+}$) = (Nb, Ti), (Sb, Ti), (Nb, Nb), have been prepared and studied. Many of the phases are new and are reported for the first time. They all show good crystallinity and the color of these compounds ranges from pure white to black depending on the (M', M'') ion combination.

The XRD patterns of the compounds were indexed on the basis of a hexagonal unit cell. The a and c lattice parameters calculated by the LSQ fit of select high angle lines are presented in Table 1. The lattice parameters of $A(Ti^{3+}, Ti^{4+})$ and the BaFeTi & BaCrTi phases are in very good agreement with those reported by Benmoussa *et al.* (12) and Masse (5), respectively. We have not noticed any monoclinic distortion in these phases. This indicates the filling of the type I site in the lattice by the alkaline earth cations. The observed increase in the c lattice parameter with the size of the A cation for the entire series of compounds also supports the filling of the type I (6b) sites situated between MO_6 octahedra along the c axis. A correlative decrease in the a lattice parameter for all the compounds has been observed. This behavior is observed in the mixed valent Ti compounds as well (12).

The experimental densities measured by pycnometry are well within 3% error of the theoretical X-ray densities obtained (Table 1), consistent with the isostructural nature of this series with Z (number of formula units/unit cell) to be 6.

The mixed valent compounds are stable under normal conditions. Long term exposure to air and moisture, however, produces surface oxidation, and hence they are usually stored in a desiccator. Thermal analysis was done for the compounds $BaTi^{3+}Ti^{4+}P_3O_{12}$, $NbTiP_3O_{12}$, and $Nb^{5+}Nb^{4+}P_3O_{12}$ in N_2 atmosphere in the temperature range 20–950°C using kaolin as the reference material at a heating rate of 10°C/min. Results show that the compounds are all stable in the measured temperature range. However, the mixed valent compounds, on heating in air or oxygen above 400°C, decompose with consequent decoloration. We found that the $Nb^{4+}Nb^{5+}P_3O_{12}$ decomposed to β-$NbPO_5$ on heating at 800°C for 12 hr and this has been confirmed by XRD. All the other compounds are stable toward exposure to air and moisture at room temperature.

B. Vibrational Spectroscopy

Table 2 lists the IR spectral assignments for the synthesized compounds in the range 1400–200 cm^{-1}. Represen-

TABLE 1
Hexagonal Lattice Parameters and Densities of $AM'^{3+}M''^{4+}P_3O_{12}$ Compounds

Compound	Color	a(Å)	c(Å)	Density (X-ray)	Density (Experimental)
$Nb^{5+}Nb^{4+}P_3O_{12}$	Black	8.648	22.42	3.389	3.39
		(8.697)	(22.12)		
$CaTi^{4+}Ti^{3+}P_3O_{12}$	Black	8.553	21.70	3.096	3.09
		(8.567)	(21.30)		
$SrTi^{4+}Ti^{3+}P_3O_{12}$	Black	8.517	22.15	3.409	3.14
		(8.488)	(21.93)		
$BaTi^{4+}Ti^{3+}P_3O_{12}$	Black	8.357	23.38	3.629	3.62
		(8.369)	(23.44)		
$CaTiCrP_3O_{12}$	Green	8.462	21.70	3.145	3.02
$SrTiCrP_3O_{12}$	Green	8.351	22.45	3.470	3.47
$BaTiCrP_3O_{12}$	Green	8.252	23.32	3.733	3.72
		(8.295)	(23.38)		
$CaTiFeP_3O_{12}$	White	8.500	21.73	3.139	3.10
$SrTiFeP_3O_{12}$	White	8.424	22.55	3.423	3.31
$BaTiFeP_3O_{12}$	White	8.277	23.38	3.776	3.80
		(8.252)	(23.30)		
$CaTiInP_3O_{12}$[a]	White	8.591	21.89	3.472	3.45
$SrTiInP_3O_{12}$[a]	White	8.529	22.73	3.723	3.74
$BaTiInP_3O_{12}$[a]	White	8.387	23.68	4.008	3.96
$CaZrCrP_3O_{12}$[a]	Green	8.626	22.11	3.273	3.14
$SrZrCrP_3O_{12}$[a]	Green	8.549	22.89	3.546	3.44
$BaZrCrP_3O_{12}$[a]	Green	8.435	23.71	3.855	3.79
$CaZrFeP_3O_{12}$[a]	White	8.649	22.11	3.286	3.33
$SrZrFeP_3O_{12}$[a]	White	8.589	22.89	3.539	3.55
$BaZrFeP_3O_{12}$[a]	White	8.484	23.76	3.829	3.83
$CaZrInP_3O_{12}$[a]	White	8.756	22.36	3.564	3.54
$SrZrInP_3O_{12}$[a]	White	8.721	23.16	3.789	3.78
$BaZrInP_3O_{12}$[a]	White	8.587	24.03	4.078	4.07

Note. Values given in parentheses are from the literature.
[a] Newly synthesized phases.

tative spectra are shown in Figs. 1–4. Factor group analysis predicts nine vibrational modes for the PO_4 unit in the NZP phases (15–17). Based on this the assignments have been made for the NZP phases that have been studied. In general, the distinguishable changes observed in the ν_3 mode (broad) for a related series of compounds could be attributed to the polarizing nature of the metal ion. The more polarizing the ion (small size, large charge; e.g., Ti^{4+}), the more localized are the electrons on the P–O(M) bond and therefore the higher will be the force constants and hence the frequencies (15).

$M^{5+}M^{4+}P_3O_{12}$(M^{5+} = Sb, Nb; M^{4+} = Ti, Nb). The IR spectra of $NbTiP_3O_{12}$ and the related metal ion incorporated phases have been studied by Subba Rao *et al.* (18). The observed spectra of $NbTiP_3O_{12}$ are in good agreement with those reported in the literature. The 1075 cm^{-1} (b) band in the Nb compound is shifted to 1085 cm^{-1} in the Sb compound due to the smaller size of Sb^{5+} compared to Nb^{5+}. The 925 cm^{-1} (m) peak could be attributed to the presence of NbO_6 octahedra rather than to the symmetric stretching vibration of the phosphate unit, on account of

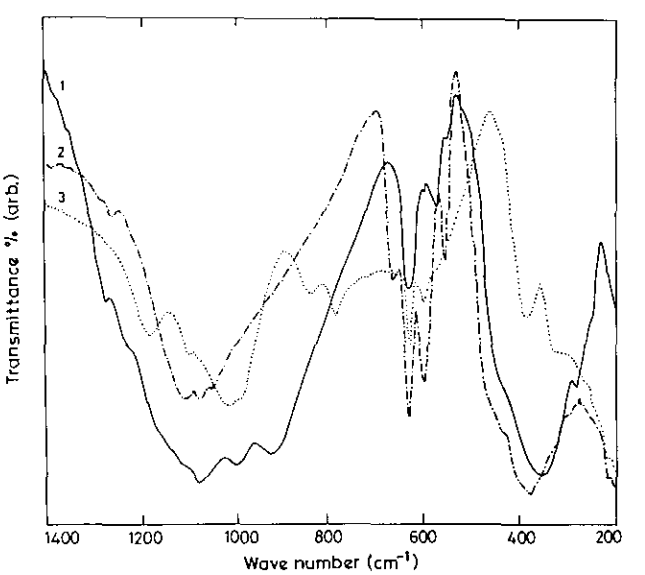

FIG. 1. IR spectra of $M^{5+}M^{4+}P_3O_{12}$: (1) $NbTiP_3O_{12}$, (2) $SbTiP_3O_{12}$, and (3) $Nb^{5+}Nb^{4+}P_3O_{12}$.

TABLE 2
Infrared Data on $AM'^{3+}M''^{4+}P_3O_{12}$ (Band Positions and Assignments in cm^{-1})

Compound	ν_3 ν_{as}(P–O)	ν_1 ν_s(P–O)	ν_4 $\delta_{(P-O)}$	ν_2 (P–O)	ν (M–O)
$NaZr_2P_3O_{12}$[a]	— 1205m 1100sh, 1050vs 1000s	920sh	650s; 584m 562m; 543sh	407sh 392w	345s
$NbTiP_3O_{12}$	1260m, 1215sh 1115b, 1075m 1000m	925m	640vs, 575s	—	360b, 280m
$SbTiP_3O_{12}$	1260m, — 1115b, 1085m, 1055w	—	660m, 632vs 603m, 551s	375b	230sh 220w
$Nb_2P_3O_{12}$	1180b, 1100m, 1025b	840m, 780b	630m, 595s	383m	325b 285sh
$CaTi_2P_3O_{12}$	— 1214m, 1184m, 1085b, 1045s	996m, 945m	655s, 570s	446m 412b	369m, 270w 245w 220w
$SrTi_2P_3O_{12}$	— 1205w, 1190w, 1085b, 1030w	955sh, 945b 740m	648s, 570s 550m	480w, 440m 392m	345w 250w 200w
$BaTi_2P_3O_{12}$	— 1200m, 1175w, 1080b, 1025	950m	665s, 640s 570s, 550m, 530s	440w	350b 240m
$SrTiCrP_3O_{12}$	— 1212sh, 1100w, 1050w	957b, 770s 738m	647s, 615w 570m, 548s	460m 400m	307w 250sh
$BaTiCrP_3O_{12}$	— 1220sh 1100w, 1010b	930w	670s, 640s 570m	460m 400b	300w 280w 250s
$CaTiFeP_3O_{12}$	— 1235b 1115m, 1004b	935b	645s, 562m	440w 389sh	362m 310w 240sh
$SrTiFeP_3O_{12}$	— 1220m, 1105b, 1002b	940b	648vs, 575sh 550s	440m 383m	360m 250m
$BaTiFeP_3O_{12}$	— 1210w, 1100m, 1000m	940m	670s, 630vs 560s	430m 380m	350m
$SrZrCrP_3O_{12}$	— 1235m, 1150b, 1120b, 1005b	970b	625vs, 600w 565s	445sh 395s	370s 246w
$BaZrCrP_3O_{12}$	— 1210sh, 1110b, 1070b, 1030b		670m, 640vs 560s	440m 380s	370s 230w
$CaZrFeP_3O_{12}$	— 1235w, 1180b, 1108w	978b	648b, 550m	445sh 394m	335b 240b
$SrZrFeP_3O_{12}$	— 1224b, 1104b, —	963b	644s, 552s	440sh 383m	329b 235w
$BaZrFeP_3O_{12}$	— 1210w, 1110b, 1070w, 1024b	975b	650vs, 560vs	432sh 387s	337s 238w 200w
$BaZrInP_3O_{12}$	—, — 1180sh, 1160b	980b, 738s	615vs, 602s 551vs, 512m	435s 385s	325b 300sh

Note. vs = very sharp, s = sharp, m = medium, w = weak, b = broad, and sh = shoulder.

[a] Values from the literature.

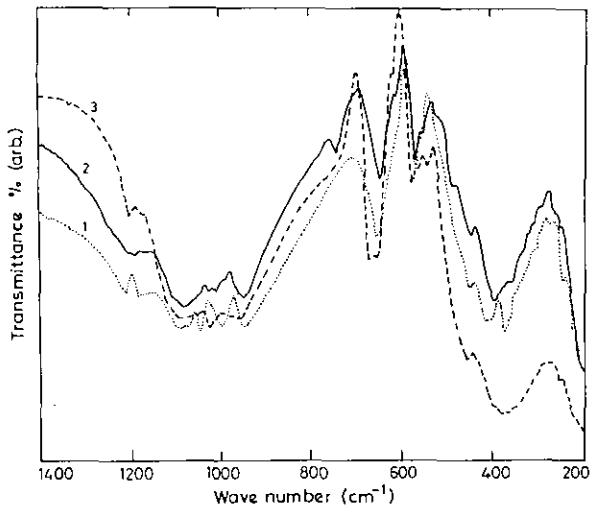

FIG. 2. IR spectra of $ATi^{4+}Ti^{3+}P_3O_{12}$: (1) A = Ca, (2) A = Sr, and (3) A = Ba.

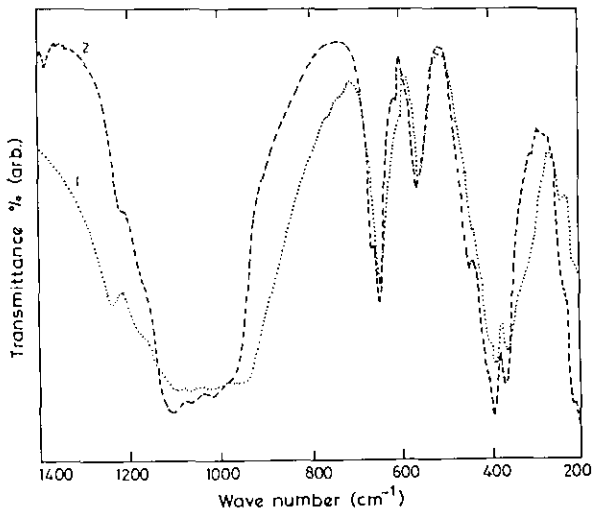

FIG. 4. IR spectra of $AZrCrP_3O_{12}$: (1) A = Sr and (2) A = Ba.

the nature of absorption. The 632 cm^{-1} band observed in the Sb compound indicates the presence of Sb in an octahedral environment of oxygen atoms (17). The covalent nature of the Ti–O bond compared to the Nb–O bond is indicated by a shift of the $\nu_{(M-O)}$ by 15–35 cm^{-1} toward the lower energy. The absorption frequencies around 550 cm^{-1} and 360–380 cm^{-1} could be attributed to the Ti–O frequencies in NbTi and SbTi compounds. The band at 840–780 cm^{-1} region in the mixed valent Nb compound indicates Nb in the octahedral site.

$ATi^{4+}Ti^{3+}P_3O_{12}$ (A = Ca, Sr, Ba). The ν_3 bands are almost identical, unlike those for the $M^{5+}M^{4+}$ series of compounds. They differ from those of NZP, indicating that the size of Ti^{3+}/Ti^{4+} is much smaller than that of Zr^{4+}. The bands in the ranges 570–550 cm^{-1} and 350–400 cm^{-1} are due to the Ti–O stretching frequencies in the TiO_6 octahedra. The number of M–O vibrations in this series decreases from Ca to Ba. This reveals the presence of distorted TiO_6 octahedra in the Ca and Sr compounds as against the presence of an almost undistorted octahedron in the Ba analogue.

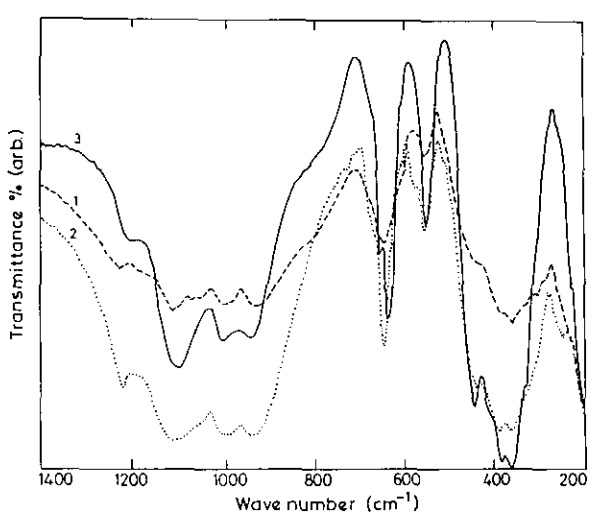

FIG. 3. IR spectra of $ATiFeP_3O_{12}$: (1) A = Ca, (2) A = Sr, and (3) A = Ba.

$ATiCrP_3O_{12}$ (A = Sr, Ba). The ν_3 band is shifted from 1000 cm^{-1} in the parent phase, NZP, to 1050 cm^{-1} and 1010 cm^{-1} in the Sr and Ba compounds, respectively. This shows the covalent nature of the Sr–O and Ba–O bonds compared to that of the Na–O bond. The bands observed in the 770–730 cm^{-1} region in the SrTiCr compound could be assigned to the vibrational modes of the CrO_6 octahedra with an out of plane deformation of O–Cr–O at 460 cm^{-1} (19).

$AMFeP_3O_{12}$ (A = Ca, Sr, Ba; M = Ti, Zr). Comparison of the ATiFe and AZrFe series in Table 2 shows conclusively the more covalent nature of the Ti–O bond compared to the Zr–O bond, since Ti^{4+} is a smaller and more polarizing ion than Zr^{4+}. Apart from the assigned PO_4 modes, the 550–560 cm^{-1} band and the 350–360 cm^{-1} band are due to the TiO_6 octahedra. The Zr–O vibrations appear at ~550–560 cm^{-1} and at 330–340 cm^{-1}, respectively (17). The 430–450 cm^{-1} region is attributed to the Fe–O vibrations. Further studies are underway in the range 400–50 cm^{-1} to characterize the A–O frequencies (A = Ca, Sr, Ba).

C. UV–Visible and DR Spectra

The UV–visible absorption and diffuse reflectance spectra (DRS) were recorded for select phases in the range 2000–200 nm. The band maxima and the transition assignments are indicated in Table 3. For comparison, the assignments of the respective metal sesquioxides and

TABLE 3
UV–Visible/DR Spectral Data

Compound	Band maxima (in cm^{-1}) in the electronic spectra of $AFe^{3+}M^{4+}P_3O_{12}$				
	$^6A_{1g} \rightarrow {}^4E_g(^4D)$	$^6A_{1g} \rightarrow {}^4T_{2g}(^4D)$	$^6A_{1g} \rightarrow ({}^4E_g + {}^4A_{1g})$	$^6A_{1g} \rightarrow {}^4T_{2g}$	$^6A_{1g} \rightarrow {}^4T_{1g}(\delta_{1f})$
$CaTiFeP_3O_{12}$	27,780	—	20,000	14,390	—
$SrTiFeP_3O_{12}$	27,780	—	20,000	14,490	—
$CaZrFeP_3O_{12}$	26,320	—	18,180	16,530	12,500
$SrZrFeP_3O_{12}$	27,030	20,830	—	14,490	12,500
Fe_2O_3	25,580	—	19,610	15,500	10,990
$LaFeO_3$	—	21,140	18,900	14,080	10,300
	Band maxima (in cm^{-1}) in the electronic spectra of Cr compounds				
Compound	Charge transfer	$^4A_{2g} \rightarrow {}^4T_{1g}(P)$	$^4A_{2g} \rightarrow {}^4T_{1g}(F)$	$^4A_{2g} \rightarrow {}^4T_{2g}(\Delta t_f)$	$^4A_{2g} \rightarrow {}^2E, {}^2T_1$
$SrTiCrP_3O_{12}$	≥36,360	—	22,730	15,390	14,820
$SrZrCrP_3O_{12}$	≥34,480	—	21,740	15,150	14,600
Cr_2O_3	39,220	27,030	21,690	16,610	14,390
$LaCrO_3$	30,500	27,400	21,510	16,260	14,600

$LaMO_3$ (M = Cr, Fe) have been given. The Cr compounds show a less intense peak at ~14,800 cm^{-1}, indicating the spin forbidden nature of the transition. The spectra for the $SrTi^{4+}Ti^{3+}P_3O_{12}$ show an absorption band around 22,220 cm^{-1} which is much broader, with a shoulder indicating the distortion of the TiO_6 octahedra.

D. Magnetic Properties

The magnetic properties of the Li-intercalated $NaTi_2P_3O_{12}$ have been reported by El Jazouli *et al.* (20). Our magnetic susceptibility data show that the compounds $ATiFeP_3O_{12}$ (A = Sr, Ba) and $BaTi^{4+}Ti^{3+}P_3O_{12}$ are paramagnetic with Curie–Weiss Law behavior (Fig. 5a). In contrast, the compounds $AZrFeP_3O_{12}$ (A = Sr, Ba) order antiferromagnetically below 10 and 13 K, respectively. Above 50 K the Curie–Weiss law is obeyed (Fig. 5b).

The effective magnetic moment μ_B and Θ are calculated and are shown in Table 4. The μ_B value for the mixed valent BaTi compound is 1.39 B.M., compared to 1.732 B.M. for the free ion. This value is in good agreement with that obtained for $LaTiO_3$ (21). This is because of the delocalization of the electron on Ti^{3+}. The observed

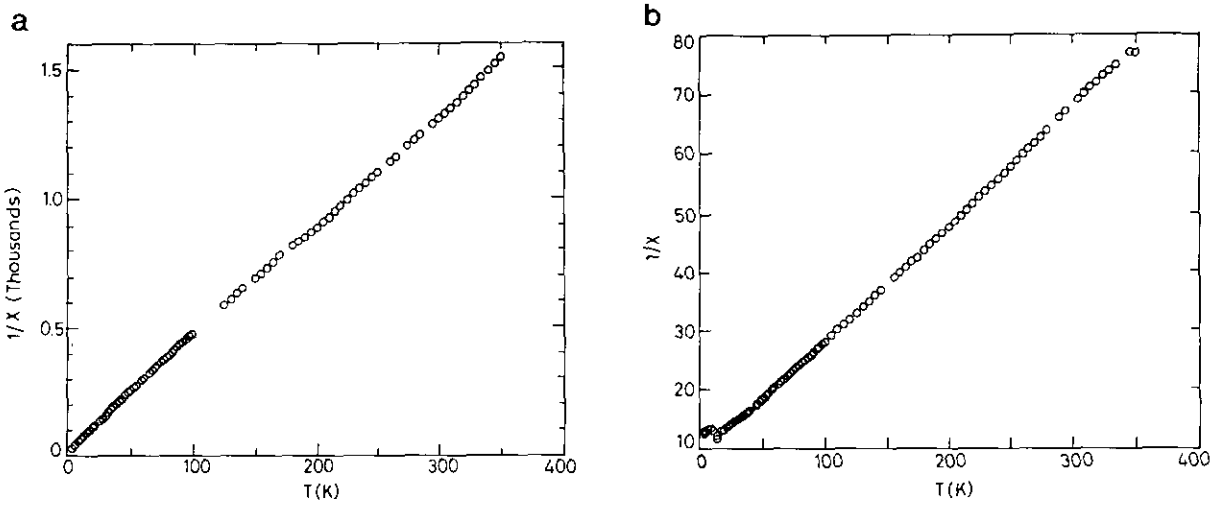

FIG. 5. Reciprocal magnetic susceptibility (χ^{-1}) vs T (a) for $BaTi^{4+}Ti^{3+}P_3O_{12}$ and (b) for $BaZrFeP_3O_{12}$.

TABLE 4
SQUID Data Measured at 1000 G

Compound	μ_{eff} B.M.	Θ K	Temperature Range K
$BaTi^{4+}Ti^{3+}P_3O_{12}$	1.39 (1.5)[a]	−16	100–350
$SrTiFeP_3O_{12}$	5.97 (5.916)[b]	−37	5–200
$BaTiFeP_3O_{12}$	5.85	−35	20–150
$SrZrFeP_3O_{12}$	5.93	−48	30–350
$BaZrFeP_3O_{12}$	6.28	−37	200–350

[a] Value computed including spin–orbit coupling.
[b] Value indicating theoretical free ion moment.

magnetic moments of the Fe^{3+} compare well with the expected free ion values.

E. EPR Studies

Electron spin resonance measurements were made on the mixed valent phosphates of the Ti series and on $Nb^{5+}Nb^{4+}P_3O_{12}$ at room temperature and at liquid N_2 temperature. No epr signal was observed at room temperature. The epr signals observed at liquid N_2 temperature are shown in Fig. 6. The results are listed in Table 5. There is a systematic variation observed in the epr signals of the mixed valent Ti compounds. The Ca compound shows two signals giving rise to anisotropic g values ($g_\perp$ and $g_|$), while in the Sr compound the two signals begin to merge. The Ba compound shows a single signal with a unique g value. This trend observed proves the presence of the distorted TiO_6 octahedra in the Ca and Sr compounds. This confirms the indication of the distortions seen in the IR spectra of the same phases (see Section B).

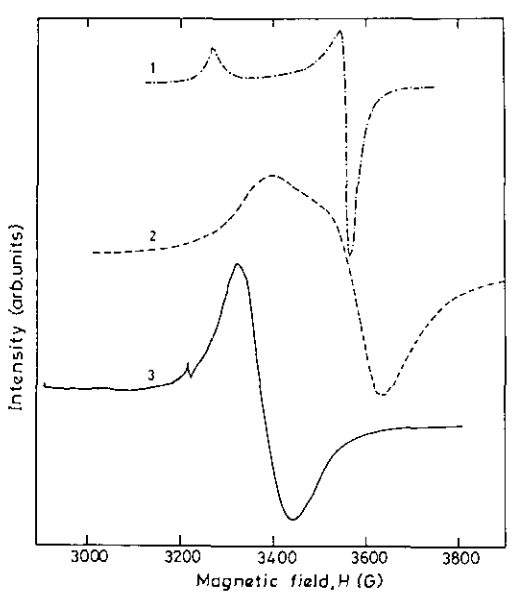

FIG. 6. EPR spectra of $ATi^{4+}Ti^{3+}P_3O_{12}$: (1) A = Ca, (2) A = Sr, and (3) A = Ba.

TABLE 5
EPR Data Collected at Liquid N_2 Temperature

Compound	$g_|$	$g_\perp$	g_{iso}
$CaTi^{4+}Ti^{3+}P_3O_{12}$	1.970	1.817	1.868
$SrTi^{4+}Ti^{3+}P_3O_{12}$	1.932	1.790	1.837
$BaTi^{4+}Ti^{3+}P_3O_{12}$	—	—	1.913
$Nb^{5+}Nb^{4+}P_3O_{12}$	—	—	1.893

CONCLUSION

A series of isostructural phosphates of NZP type phase have been synthesized, characterized by X-ray diffraction, density, spectroscopic techniques, and magnetic studies. Thermal expansion and dielectric constant measurements are under way and will be reported elsewhere.

ACKNOWLEDGMENT

Thanks are due to BRNS, Bombay, for the award of a research grant.

REFERENCES

1. P. Vashista, J. M. Mundy, and G. K. Shenoy (Eds.), "Fast Ion Transport in Solids: Electrodes and Electrolytes." North-Holland, New York, 1979; P. Hagenmuller and W. Van Gool (Eds.), "Solid Electrolytes." Academic Press, New York, 1978; B. V. R. Chowdari and S. Radhakrishna (Eds.), "Materials for Solid State Batteries." World Science, Singapore, 1986.
2. C. N. R. Rao and J. Gopalakrishnan, "New Directions in Solid State Chemistry." Cambridge Univ. Press, Cambridge, 1986.
3. C. Delmas, A. Nadiri, and J. L. Soubeyroux, *Solid State Ionics* **28–30,** 419 (1988); J. B. Goodenough, H. Y-P. Hong, and M. Kafalas, *Mater. Res. Bull* **11,** 203 (1976); B. A. Taylor, A. D. English, and T. Berzins, *Mater. Res. Bull.* **12,** 171 (1977).
4. L. O. Hagman and P. Kierkegaard, *Acta Chim. Scand.* **22,** 1822 (1968); M. Sljukic, B. Matkovic, and B. Prodic, *Z. Kristallogr.* **130,** 148 (1969).
5. R. Masse, *Bull. Soc. Fr. Mineral. Cristallogr.* **95,** 405 (1972); Boudjada, Abdelhamid, and Perret Rene, *C.R. Hebd. Seances Acad. Sci. Ser. C.* **281**(1), 31, (1975).
6. A. El Jazouli, J. L. Soubeyroux, J. M. Dance, and G. Le Flem, *J. Solid State Chem.* **65,** 351 (1986).
7. J. L. Rodrigo and J. Alamo, *Mater. Res. Bull.* **26,** 475 (1991).
8. L. Bennouna, M. R. Lee, R. Brochu, and M. Quarton, *C.R. Acad. Sci. Paris Ser. II* **310,** 727 (1990).
9. J. Gopalakrishnan and K. Kasturirangan, *Chem. Mater.* **4,** 745 (1992); U. V. Varadaraju, K. A. Thomas, B. Sivasankar, and G. V. Subba Rao, *J. Chem. Soc. Chem. Commun.* **11,** 814 (1987).
10. R. Masse, A. Durif, and J. Guitel, *Bull. Soc. Fr. Mineral. Cristallogr.* **95,** 47 (1972).
11. A. Leclaire, M. M. Borel, A. Grandin, and B. Raveau, *Acta Crystallogr. Sect. C* **45,** 699 (1989).
12. A. Benmoussa, M. M. Borel, A. Grandin, A. Leclaire, and B. Raveau, *Ann. Chim. Fr.* **14,** 181 (1989).
13. Rustom Roy, D. K. Agrawal, J. Alamo, and R. A. Roy, *Mater.*

Res. Bull. **19,** 699 (1984); S. Shenbhagaraman and A. M. Umarji, *J. Solid State Chem.* **85,** 169 (1990).
14. T. Oota and I. Yamai, *J. Am. Ceram. Soc.* **69,** 1 (1986).
15. M. Barj, H. Perthuis, and Ph. Colomban, *Solid State Ionics* **11,** 157 (1983); M. Barj, H. Perthuis, and Ph. Colomban, *Solid State Ionics* **9–10,** 845 (1983).
16. A. Mbandza, E. Bordes, and P. Courtine, *Mater. Res. Bull.* **20,** 251 (1985).
17. Kazuo Nakamoto, "Infrared and Raman Spectra of Inorganic and Coordination Compounds." Wiley, New York, 1978; R. A. Nyquist and R. O. Kagel, "Infrared Spectra of Inorganic Compounds." Academic Press, New York, 1971.
18. G. V. Subba Rao, U. V. Varadaraju, K. A. Thomas, and B. Sivasankar, *J. Solid State Chem.* **70,** 101 (1987).
19. G. V. Subba Rao and C. N. R. Rao, *Appl. Spectrosc.* **24,** 436 (1970).
20. El Jazouli, A. Nadiri, J. M. Dance, C. Delmas, and G. Le Flem., *J. Phys. Chem. Solids* **49,** 779 (1988).
21. J. Sieler and H. Hennig, *J. Prakt. Chem.* **34,** 168 (1966).